



2 **Can thin cirrus clouds in the tropics provide a**  
 3 **solution to the faint young Sun paradox?**

4 Roberto Rondanelli<sup>1,2</sup> and Richard S. Lindzen<sup>1</sup>

5 Received 13 March 2009; revised 8 September 2009; accepted 22 September 2009; published XX Month 2010.

6 [1] In this paper we present radiative-convective simulations to test the idea that tropical  
 7 cirrus clouds, acting as a negative feedback on climate, can provide a solution to the faint  
 8 young Sun paradox. We find that global mean surface temperatures above freezing can  
 9 indeed be found for luminosities larger than about 0.8 (corresponding to ~2.9 Ga and  
 10 nearly complete tropical cirrus coverage). For luminosities smaller than 0.8, even though  
 11 global mean surface temperatures are below freezing, tropical mean temperatures are still  
 12 above freezing, indicating the possibility of a partially ice-free Earth for the Early  
 13 Archean. We discuss possible mechanisms for the functioning of this negative feedback.  
 14 While it is feasible for tropical cirrus to completely eliminate the paradox, it is similarly  
 15 possible for tropical cirrus to reduce the amounts of other greenhouse gases needed  
 16 for solving the paradox and therefore easing the constraints on CO<sub>2</sub> and CH<sub>4</sub> that appear to  
 17 be in disagreement with geological evidence.

18 **Citation:** Rondanelli, R., and R. S. Lindzen (2010), Can thin cirrus clouds in the tropics provide a solution to the faint young Sun  
 19 paradox?, *J. Geophys. Res.*, 115, XXXXXX, doi:10.1029/2009JD012050.

21 **1. Introduction**

22 [2] Models for the evolution of the Sun during the main  
 23 sequence call for a reduced solar luminosity and therefore a  
 24 reduced Earth's solar constant of about  $S = 0.75 S_0$  around  
 25 3.8 Ga (with  $S_0$  the present solar constant ~1353 W/m<sup>2</sup>)  
 26 [Schwarzschild, 1958; Newman and Rood, 1977]. At the same  
 27 time, geological evidence shows the presence of a  
 28 stable ocean and liquid water in the planet at least after  
 29 3.9 Ga (and perhaps even earlier [e.g., Wilde et al., 2001;  
 30 Pinti, 2005]). The fact that simple models of the Earth's  
 31 climate cannot reconcile the reduced luminosity with the  
 32 presence of liquid water (and the absence of glacial deposits)  
 33 has become known as the faint young Sun paradox [Sagan  
 34 and Mullen, 1972]. The paradox hinges on the assumption  
 35 of a constant atmospheric composition or, more precisely,  
 36 on the assumption of a constant atmospheric greenhouse  
 37 effect and a constant atmospheric solar reflectivity (both  
 38 including gases and clouds). Just for illustration purposes,  
 39 one can use a crude zero-dimensional energy balance for the  
 40 atmosphere to calculate the mean global surface temperature  
 41 ( $T_s$ ) [e.g., Catling and Kasting, 2007],

$$T_s = T_g + \left( \frac{(1-A)S}{4\sigma} \right)^{\frac{1}{4}}, \quad (1)$$

43 where  $A$  is the planetary albedo and  $T_g$  is a temperature that  
 44 encapsulates the greenhouse effect of the atmosphere and

clouds. For current climate with  $A = 0.3$  and  $T_g = 34$ ,  $T_s = 45$   
 288 K. According to the standard solar model, the 46  
 luminosity, and therefore the variation of the solar constant 47  
 can be approximated by [Gough, 1981] 48

$$S = \frac{S_0}{1 + 0.4t/4.6}, \quad (2)$$

where  $t$  is the time in Ga. 50

[3] Under the assumption of a constant greenhouse effect, 51  
 the simple zero-dimensional model gives  $T_s = 269$  K for a 52  
 solar luminosity of  $S = 0.75 S_0$ , ~ 3.9 Ga.  $T_s$  rises above 53  
 freezing for  $S \sim 0.79 S_0$ , which corresponds to 2.9 Ga. It 54  
 might seem that a much reduced value of  $A$  in equation (1) 55  
 could increase the temperature above freezing. However, 56  
 the absence of clouds (the main driver of the albedo) would 57  
 also result in a significant reduction of the greenhouse 58  
 effect. A first correction to the simple model is to include 59  
 a water vapor feedback by assuming a constant relative 60  
 humidity (instead of the implicit assumption of constant 61  
 specific humidity). By including this positive water vapor 62  
 feedback in a 1-D radiative convective model one increases 63  
 the time range of the paradox: a colder surface temperature 64  
 implies a drier atmosphere and a reduced greenhouse effect. 65  
 For instance, Kasting et al. [1988] found that  $T_s$  remains 66  
 below freezing up until ~2 Ga or  $S \sim 0.85 S_0$ . Moreover, 67  
 Pierrehumbert [2010] shows that including an ice-albedo 68  
 feedback the paradox is even more dramatic and the 69  
 solution for  $S = 0.75 S_0$  is a snowball Earth with  $T_s = 70$   
 228 K (however, see Cogley and Henderson-Sellers [1984] 71  
 for arguments on a much reduced role for the ice-albedo 72  
 feedback on the early Earth). 73

[4] Sagan and Mullen [1972] first pointed out the exis- 74  
 tence of the paradox and suggested that trace amounts of 75

<sup>1</sup>Department of Earth, Atmospheric and Planetary Sciences, Massachusetts Institute of Technology, Cambridge, Massachusetts, USA.

<sup>2</sup>Department of Geophysics, University of Chile, Santiago, Chile.

76 NH<sub>3</sub> could solve the paradox. This solution was later found  
 77 untenable due to the relatively small lifetime of NH<sub>3</sub> to  
 78 photolysis in an anoxic atmosphere [Kuhn and Atreya,  
 79 1979]. Most of the solutions to the paradox have relied on  
 80 changes in  $T_g$  produced by either CO<sub>2</sub>, CH<sub>4</sub> or both [e.g.,  
 81 Hart, 1978; Owen et al., 1979; Kasting, 1987; Kasting et  
 82 al., 1988; Pavlov et al., 2000; Haqq-Misra et al., 2008].  
 83 Solutions that involve high CO<sub>2</sub> atmospheric concentrations  
 84 are particularly appealing given the existence of large  
 85 reservoirs of carbon in the Earth's mantle and continents  
 86 (and the relative smallness of the atmospheric and oceanic  
 87 reservoirs). The temperature dependence of the silicate  
 88 weathering rate (mainly through the temperature dependence  
 89 of the precipitation) can act as a negative feedback on climate  
 90 acting through the CO<sub>2</sub> geological cycle [Walker et al., 1981].  
 91 According to this mechanism, climates colder than present  
 92 are expected to have a higher CO<sub>2</sub> concentrations, compen-  
 93 sating to some extent for the reduced solar luminosity.

94 [5] However, some geological evidence from paleosols  
 95 and other proxies indicates that CO<sub>2</sub> concentrations must be  
 96 at least ten times smaller than those required to produce  
 97 mean surface temperatures above freezing in 1-D radiative-  
 98 convective models [Rye et al., 1995; Rollinson, 2007].  
 99 Zahnle and Sleep [2002] also argue on the basis of theo-  
 100 retical calculations of the carbon geological cycle, that high  
 101 CO<sub>2</sub> concentrations are implausible. If the geological evi-  
 102 dence is taken at face value, the paradox seems to be  
 103 unresolved [Shaw, 2008]. This realization has prompted  
 104 even the reconsideration of the relevance of the standard  
 105 model for solar evolution and therefore the faintness of the  
 106 early Sun [e.g., Sackmann and Boothroyd, 2003]. However,  
 107 evidence for the standard solar model is strong. In partic-  
 108 ular, solar analogs appear to show no evidence for the  
 109 magnitude and time scale of mass loss required to explain  
 110 an early bright Sun [Minton and Malhotra, 2007].

111 [6] The meridional heat transport can also change under  
 112 different forcing conditions, potentially providing a stabi-  
 113 lizing influence on climate, specially for the onset of  
 114 snowball solutions [e.g., Lindzen and Farrell, 1980]. The  
 115 moderating influence of meridional heat transport has been  
 116 discussed in the context of the faint young Sun paradox by  
 117 Endal and Schatten [1982], who proposed a much more  
 118 effective ocean heat transport in an early Earth with small  
 119 continents. However, a more effective heat transport would  
 120 also produce a larger value for the critical insolation for the  
 121 onset of a snowball Earth. Gerard et al. [1990], based on the  
 122 maximum entropy principle [Paltridge, 1978], deduced that  
 123 the heat transport becomes less efficient for lower solar  
 124 luminosities and therefore they obtain solutions that are  
 125 stable to an ice-albedo feedback for the whole evolution of  
 126 the solar constant.

127 [7] Besides purely dynamical or radiative mechanisms to  
 128 account for the moderate temperatures under lower solar  
 129 luminosity, the rise of life and subsequent changes in  
 130 atmospheric composition may have played a role in the  
 131 climate stabilization required to explain the paradox. For  
 132 instance, the rise of early bacteria could have increased  
 133 methane fluxes into an early anoxic atmosphere [e.g.,  
 134 Pavlov et al., 2000] providing methane concentrations of  
 135 about 100 times present concentrations [Pavlov et al.,  
 136 2003]. The enhancement of the weathering rate due to the  
 137 rise of life has also been proposed as a negative feedback on

climate [Volk, 1987; Schwartzman and Volk, 1989, 2004] 138  
 and moreover as a potential self-regulating mechanism for 139  
 the biosphere [Lovelock and Whitfield, 1982]. 140

[8] Water clouds on the other hand, have been only rarely 141  
 invoked as a possible solution to the paradox, although 142  
 changes in their composition, height and areal extent can 143  
 potentially provide large changes in both  $A$  and  $T_g$ . When 144  
 studying the effect of greenhouse gases, clouds properties 145  
 are usually kept constant. The rationale and limitations for 146  
 the assumption of constant cloud properties are summarized 147  
 by Kasting and Catling [2003]: "If the goal is to determine 148  
 what is required to create a climate similar to that of today, it 149  
 is reasonable to assume no change in cloud properties. For 150  
 model planets that are either much hotter or much colder 151  
 than present Earth, however, the neglect of cloud feedback 152  
 may lead to serious error." The matter of how much colder 153  
 (or hotter) a climate should be so that the effect of cloud 154  
 feedbacks becomes important has been the subject of some 155  
 previous studies on the role of clouds in the early Earth 156  
 climate [Henderson-Sellers and Cogley, 1982; Rossow et 157  
 al., 1982]. In those studies a decrease in cloud liquid water 158  
 in colder climates is associated with a decrease in planetary 159  
 albedo large enough to produce mean global surface tem- 160  
 peratures above freezing for  $S \gtrsim 0.8 S_0$ . 161

[9] Here, we focus on testing the feasibility of a solution 162  
 based on changes in the cirrus cloud coverage in the tropics. 163  
 We are primarily interested whether a plausible change in 164  
 the coverage of thin cirrus clouds can solve the faint young 165  
 Sun paradox, regardless of the origin of such a change. We 166  
 focus on tropical cirrus clouds because contrary to extra- 167  
 tropical clouds, in which cloud coverage is mostly related to 168  
 the relative area of ascent and descent in baroclinic dis- 169  
 turbances, the mechanism of formation of cirrus in the 170  
 tropics appears to be particularly susceptible to a surface 171  
 temperature dependence. An example of a mechanism that 172  
 could relate sea surface temperature to thin cirrus cloud 173  
 coverage is the iris hypothesis proposed by Lindzen et al. 174  
 [2001]. We defer to section 4 the discussion of this 175  
 particular mechanism. 176

[10] Thin cirrus clouds are a ubiquitous feature of the 177  
 current tropical atmosphere. Recent global data using sat- 178  
 ellite lidar and radar instruments place the frequency of thin 179  
 cirrus clouds ( $\tau < 3-4$ ) at  $\sim 25\%$  over the tropics ( $30^\circ\text{S}-$  180  
 $30^\circ\text{N}$ ) [Sassen et al., 2008]. Trajectory studies show that at 181  
 least two mechanisms explain the formation of cirrus clouds 182  
 in the tropics; a direct detrainment from convective clouds 183  
 and also a triggering by gravity waves further away from the 184  
 original convective region [Mace et al., 2006]. Although 185  
 cirrus clouds are believed to have a net positive radiative 186  
 effect, there remains uncertainty on this point [Liou, 2005]. 187  
 Nevertheless, recent satellite estimations of the cloud radi- 188  
 ative effect of cirrus clouds [Choi and Ho, 2006] seem to 189  
 confirm the long-held idea that thin cirrus clouds (that is 190  
 clouds with visible optical depths  $\tau \lesssim 10$ ) have a much 191  
 larger infrared heating effect than a shortwave cooling, and 192  
 therefore a strong positive cloud radiative effect. 193

[11] One-dimensional radiative convective simulations, 194  
 including at least some representation of cirrus clouds, have 195  
 already shown the potential of thin cirrus clouds to produce 196  
 significant surface warming. In the seminal paper by Manabe 197  
 and Wetherald [1967], the addition of a layer of full black 198  
 cirrus cloud was enough to increase the equilibrium surface 199

200 temperature from 280 K to 320 K. Similarly, *Liou and*  
 201 *Gebhart* [1982] show radiative-convective equilibrium sim- 258  
 202 ulations in which the inclusion of a thin cirrus cloud can 259  
 203 increase surface temperatures to  $\sim 320$  K for total coverage, 260  
 204 with the surface temperature being relatively independent of 261  
 205 the height of the cloud base. In the next sections, we present 262  
 206 results from a simple radiative-convective model in which 263  
 207 the tropical thin cirrus cloud coverage ( $f$ ) is specified. 264

## 208 2. Model Assumptions

209 [12] The 1-D model is a simple radiative-convective 265  
 210 equilibrium model based on the original formulation by 266  
 211 *Manabe and Strickler* [1964] and *Manabe and Wetherald* 267  
 212 [1967]. The model has 140 levels in pressure from 1000 hPa 268  
 213 to 0.04 hPa, following the sigma-level pressure coordinates 269  
 214 defined by *Manabe and Wetherald* [1967]. The model is run 270  
 215 for 600 days from an initial moist adiabatic atmosphere with 271  
 216 surface temperature of 300 K, with time step of 1 day 272  
 217 (equilibrium between incoming shortwave and outgoing 273  
 218 longwave radiation is reached within less than  $1 \text{ W/m}^2$ ). 274  
 219 We use a similar relative humidity profile as in *Manabe and* 275  
 220 *Wetherald* [1967] with a surface relative humidity of 0.8 and 276  
 221 a constant stratospheric water vapor mixing ratio of  $3 \times$  277  
 222  $10^{-6}$ . At each time step we use solar and infrared radiative 278  
 223 parameterizations (developed for general circulation models 279  
 224 [*Chou and Suarez*, 2002; *Chou et al.*, 2003]) to estimate the 280  
 225 radiative heating rates in each vertical layer. A convective 281  
 226 adjustment is performed at each time step, so unstable layers 282  
 227 are adjusted to a reversible moist adiabat (which at least for 283  
 228 the tropics seems to be a very good approximation for the 284  
 229 temperature vertical distribution [*Emanuel*, 2007]). In all the 285  
 230 runs, unless otherwise noted, the concentration of the 286  
 231 radiatively active gases (except for water vapor) is kept 287  
 232 fixed and approximately equal to the present atmospheric 288  
 233 levels (PAL). That is,  $\text{CO}_2 = 350$  ppmv and  $\text{CH}_4 = 1.75$  ppmv. 289

234 [13] We assess the effect of the coverage of tropical cirrus 290  
 235 clouds on surface temperature with some very simple 291  
 236 assumptions. The effect of clouds other than thin cirrus 292  
 237 (hereafter  $\tau < 9$ ) is not explicitly incorporated, but rather 293  
 238 enters as a constant planetary albedo fixed to about 0.2 (this 294  
 239 is only part of the planetary albedo, since the radiative 295  
 240 parameterization calculates explicitly the scattering by the 296  
 241 clear atmosphere and thin cirrus clouds). In this way an 297  
 242 incoming solar radiation and a coverage of 0.16 for thin 298  
 243 cirrus, will provide a surface temperature close to the 299  
 244 observed in the present (298 K for the mean tropical 300  
 245 temperature). The incoming solar radiation that provides 301  
 246 the current tropical average temperature ( $\sim 285 \text{ W/m}^2$  after 302  
 247 correcting by the solar zenith angle and constant planetary 303  
 248 albedo), will serve as a basis for changing the solar constant 304  
 249 in the model, mimicking the solar history. The solar zenith 305  
 250 angle is kept constant and equal to  $60^\circ$ . The treatment of 306  
 251 clouds in the radiative parameterization is explained in 307  
 252 detail by *Chou and Suarez* [2002]; *Chou et al.* [2003]. 308  
 253 The cloud optical thickness in the visible spectral region 309  
 254 ( $\tau_c$ ) is a function of both the effective radius of the cloud 310  
 255 particles  $r_e$  and the ice water path (IWP) of the cloud, and it 311  
 256 is parameterized as 312

$$\tau_c = \text{IWP} \frac{1.64}{r_e}, \quad (3)$$

where IWP has units of  $\text{g m}^{-2}$  and  $r_e$  has units of  $\mu\text{m}$ . The 258  
 parameterization of the cloud radiative effect in the visible 259  
 is independent of the solar spectral bands. The value of  $r_e$  is 260  
 calculated according to the empirical regression by 261  
*McFarquhar* [2001] as a function of both the local 262  
 temperature and the value of the cloud water content. The 263  
 parameterization of the infrared optical depth of the cloud, 264  
 takes into account the absorption and scattering of radiation 265  
 by the cloud [*Chou et al.*, 1999]. The extinction coefficient, 266  
 the single scattering albedo and the asymmetry factor are all 267  
 dependent on  $r_e$  and on the particular spectral band [*Chou et* 268  
*al.*, 2003]. By specifying the thickness of the cloud (here 269  
 equal to one model vertical layer) and by specifying the 270  
 cloud water content, both IWP and  $r_e$  can be calculated. 271

[14] In the control case, we specify the value of cloud 272  
 liquid water content to  $7 \times 10^{-4} \text{ g/g}$ , so that a cloud with a 273  
 thickness of 9 hPa results in an IWP  $\sim 44 \text{ g/m}^2$ . The cloud 274  
 is first located at a fixed level of 200 hPa (we will discuss 275  
 the effect of relaxing this assumption to make it consistent 276  
 with the changes in the vertical temperature structure over 277  
 the range of solar forcings). We use a single cloud as a 278  
 proxy for the radiative effect of all types of thin cirrus 279  
 clouds in the tropics. The selection of this particular cloud is 280  
 not arbitrary, rather it is such that it roughly matches the 281  
 radiative forcing from observations in current climate as 282  
 estimated by *Choi and Ho* [2006]. For the control run, the 283  
 selected cloud provides a longwave cloud radiative effect of 284  
 $+115 \text{ W/m}^2$  and a shortwave cloud radiative effect of 285  
 $-50 \text{ W/m}^2$ . These values coincide roughly with the observed 286  
 values derived by *Choi and Ho* [2006] for both the long- 287  
 wave and the shortwave radiative effect as well as the net 288  
 positive cloud radiative effect of these clouds, which is 289  
 about  $+46 \text{ W/m}^2$  for all clouds with  $\tau < 4$ . 290

## 291 3. Results

### 292 3.1. Single Column Radiative-Convective Simulation

[15] In the first run we explore the behavior of the tropical 293  
 surface temperature in radiative convective equilibrium for 294  
 different values of the thin cirrus cloud coverage. Figure 1a 295  
 shows the results for this tropics-only column. For the 296  
 current solar insolation  $S_0$  and current cloud coverage  $f \sim$  297  
 $0.16$  the surface temperature is  $\sim 298$  K. An increase in the 298  
 coverage of this thin cirrus cloud from  $f = 0.16$  to  $f = 1$  299  
 would produce an increase in the surface temperature in the 300  
 tropics to about 325 K. From Figure 1a, we notice that the 301  
 mean tropical temperature is above freezing for constant 302  
 atmospheric conditions (lower gray line), even at solar 303  
 insolutions of about  $S \sim 0.81 S_0$ . We note that the usual 304  
 statement of the faint young Sun paradox is made in terms 305  
 of mean surface temperature. Therefore a solution is con- 306  
 sidered as such when the mean surface temperature is above 307  
 freezing (hereafter, this is what we will consider a solution). 308  
 A weaker version of the paradox can be envisioned in which 309  
 temperatures are above freezing for a significantly large area 310  
 of the planet. One can also envision a stronger version of the 311  
 paradox in which one takes the absence of evidence of 312  
 glaciation as an indication of a completely ice-free Earth. 313

[16] The three black dashed lines in Figures 1a–1d 314  
 represent three different relative rates of change for the thin 315  
 cirrus cloud coverage (so a  $-10\%/K$  rate of change repre- 316  
 sents a change from 0.16 to 0.176 from 298 K to 297 K. We 317

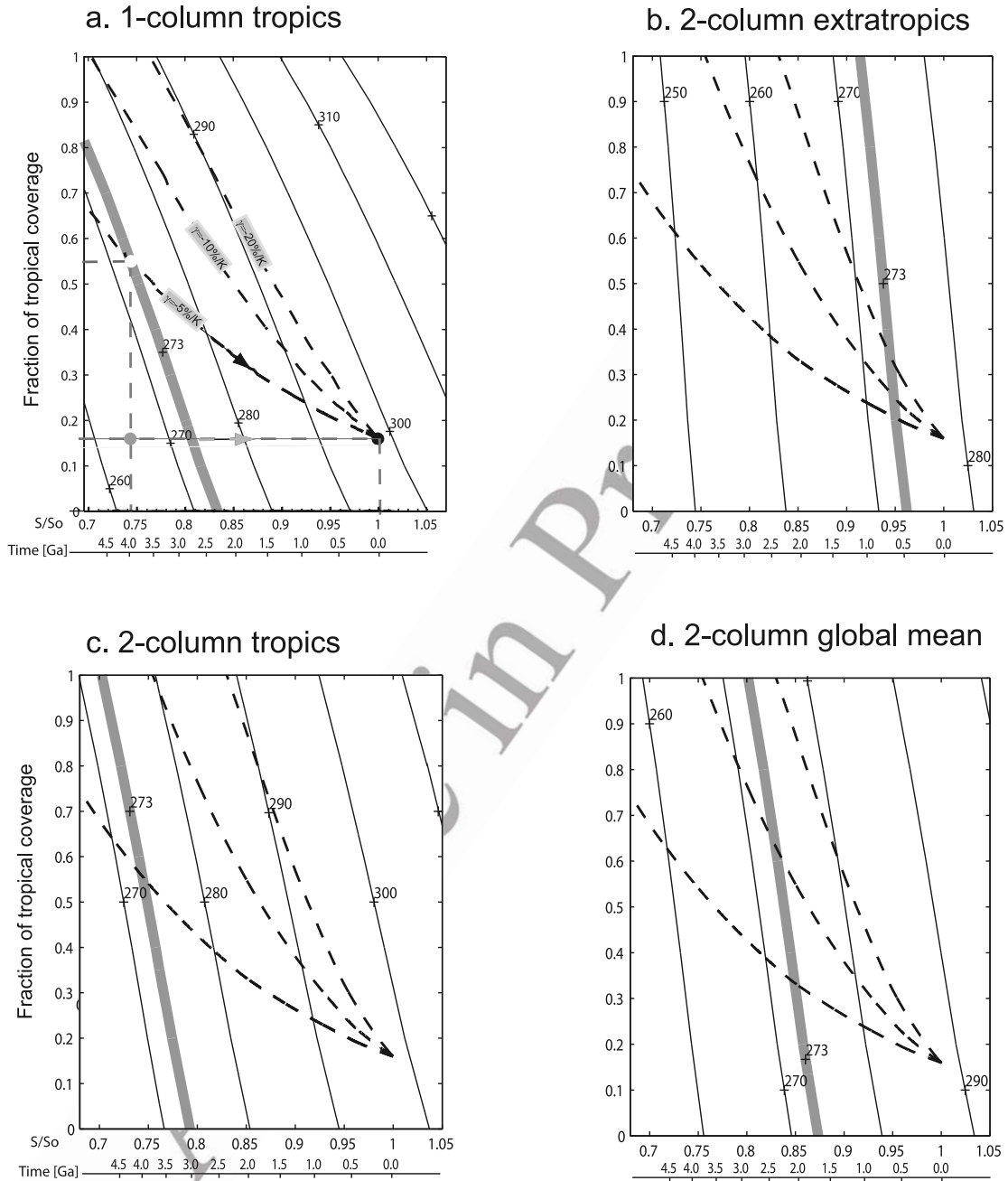


**Figure 1.** Equilibrium surface temperature corresponding to (a) one-column, tropics-only simulation, (b) extratropical column in the two-column simulation, (c) tropical column in the two-column simulation, and (d) global mean in the two-column simulation. The temperature is indicated by the solid black lines. In Figure 1a a black dot indicates current climate conditions. The white dot indicates the climate surface temperature corresponding to a luminosity of  $\sim 0.74S_0$  and a cloud coverage of 0.55. This climate occurs for a rate of change of  $-5\%/K$  in the coverage of thin cirrus clouds in the tropics. The two other dashed lines represent rates of change in the cloud coverage of  $-10\%/K$  and  $-20\%/K$  as labeled. The grey dot is the equilibrium temperature of a climate with the same luminosity as the white dot but with no cloud feedback. The time scale in the abscissa is calculated according to equation (2).

318 will denote this rate of change as  $\gamma = \frac{1}{f} \frac{\partial f}{\partial T_t}$ , where  $T_t$  is the  
 319 mean tropical rate. The rate of change  $\gamma$  represents implicitly the magnitude of the climate feedback associated with  
 320 increase in thin cirrus clouds. The dashed lines in each of the panels of Figure 1 are for magnitudes of  $\gamma = -5\%/K$ ,  
 321  $-10\%/K$  and  $-20\%/K$ . For this tropics-only case, to sustain  
 322 surface temperatures above freezing for  $S = 0.7 S_0$ , one  
 323  
 324

would need a cirrus coverage of about 0.8. This surface  
 325 coverage is accomplished with a mere  $-6\%/K$  change in the  
 326 cloud coverage.  
 327

### 3.2. Two-Column Radiative-Convective Simulation 328

[17] Since in the previous simulation we only deal with a  
 329 tropical column, we cannot test the paradox in its more  
 330

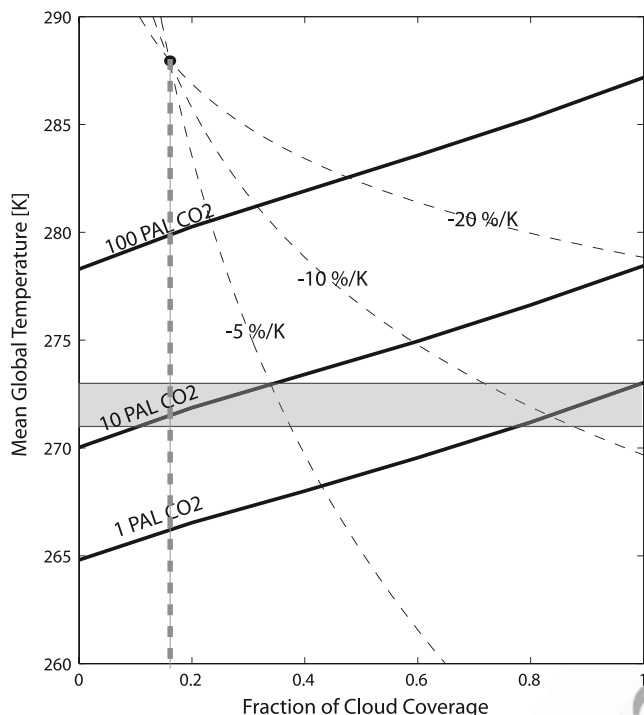


**Figure 2.** Mean surface temperature corresponding to the two-column radiative convective model for  $S = 0.8S_0$ . The black solid lines are three different concentrations of  $\text{CO}_2$  (PAL stands for present atmospheric level). The dashed lines represent different rates of change in the thin cirrus cloud coverage from the present value of 0.16. The gray horizontal strip is meant to represent a range of temperatures for freezing water between 271 and 273 K.

331 usual framing, that is, with respect to global mean temper-  
 332 ature. Also, since the incoming solar radiation in the single  
 333 column has been tuned so as to produce the observed  
 334 current tropical temperature, the heat transported out of  
 335 the tropical column (implicit in the tuning) decreases in  
 336 the same proportion as the solar insolation.

337 [18] We add an extratropical column to the model and we  
 338 will assume a diffusive heat transport between the two  
 339 columns, with a constant transport coefficient  $K = 3 \times$   
 340  $10^6 \text{ m}^2/\text{s}$  over the depth of the model, so that at each time  
 341 step, the temperature in each layer is calculated as the sum  
 342 of three tendencies; the radiative heating, the convective  
 343 adjustment and the meridional transport between the  
 344 columns.

345 [19] The results for the two-column simulations are  
 346 shown in Figures 1b, 1c and 1d. Figure 1c can be directly  
 347 compared to Figure 1a. We see that assumption of a  
 348 diffusive transport makes the two-column tropics warmer  
 349 than the single-column tropics for low cirrus coverages ( $f \lesssim$   
 350 0.45), and colder for relatively high coverages. Since no  
 351 change other than the cirrus coverage in the tropical column  
 352 is made, all change in temperature with cloud coverage in  
 353 the extratropical column shown in Figure 1b is due to the  
 354 transport from the tropical column. Figure 1d shows the  
 355 global mean surface temperature (calculated as simply the  
 356 average between the surface temperature in the two col-

umns). We see that for constant atmospheric composition 357  
 (that is following a line of constant  $f = 0.16$  in Figure 1d) the 358  
 global mean surface temperature in our two-column model 359  
 remains below freezing up until  $S = 0.86 S_0$  giving some- 360  
 what warmer temperatures than with previous 1-D radiative- 361  
 convective simulations ( $\sim 265 \text{ K}$  at  $S = 0.8 S_0$  compared to 362  
 $\sim 262 \text{ K}$  for the same insolation as in work by *Haqq-Misra* 363  
*et al.* [2008]). We are confident that these differences are not 364  
 due to the peculiarities of the radiative parameterization or 365  
 to the convective adjustment since our own 1-D tropical 366  
 simulations with no cloud cover can be used to recover a 367  
 temperature of about  $263 \text{ K}$  for  $S = 0.8 S_0$  similar to the ones 368  
 reported for current atmospheric composition at  $S = 0.8 S_0$  369  
 [Kasting and Catling, 2003; *Haqq-Misra et al.*, 2008]. 370

[20] The dashed curves in Figure 1d indicate that for 371  
 some value of  $\gamma$  between  $-10\%/K$  and  $-20\%/K$ , there is a 372  
 solution of the paradox up to  $S = 0.8 S_0$  or for a the range 373  
 between 2.9 and 1.9 Ga. This solution would imply a total 374  
 cirrus coverage for the tropics, and a tropical mean temper- 375  
 ature of about  $285 \text{ K}$ . A smaller rate of change of about 376  
 $-7\%/K$  however, can sustain global mean temperatures of 377  
 only  $\sim 261 \text{ K}$  for  $S = 0.72 S_0$ , although tropical mean 378  
 surface temperatures in this case would be just above 379  
 freezing, suggesting that even this moderate rate of change 380  
 in cloud coverage could explain ice-free conditions for large 381  
 regions of Earth. 382

### 3.3. Thin Cirrus and Increased Greenhouse Gases 383

[21]  $\text{CO}_2$  alone can provide enough greenhouse effect to 384  
 overcome the paradox. However, geological evidence seems 385  
 to point to less  $\text{CO}_2$  present in the atmosphere than would 386  
 be required. For instance, *Rye et al.* [1995] argue on the 387  
 basis of the absence of siderite that  $\text{CO}_2$  concentrations 388  
 higher than about 10 times the present atmospheric level 389  
 (10 PAL) at  $273 \text{ K}$  are unlikely at about 2.8 Ga ( $S \sim 0.81 S_0$ ). 390  
 This limit is temperature-dependent and goes up to about 391  
 $50 \text{ PAL}$  at temperatures above  $300 \text{ K}$ . *Kasting* [1993] quotes 392  
 levels of  $\text{CO}_2$  that are several times higher than the paleosol 393  
 limit ( $\sim 50 \text{ PAL}$  for reaching  $T_s \sim 273 \text{ K}$  for  $S = 0.8 S_0$ ). The 394  
 discrepancy between required and estimated  $\text{CO}_2$  concen- 395  
 trations is also found in other geological and theoretical 396  
 evidence [see, e.g., *Rollinson*, 2007, and references therein]. 397  
 $\text{CH}_4$ , with a much longer lifetime in an anoxic atmosphere 398  
 than in the present atmosphere, could provide an additional 399  
 greenhouse effect. However, recent calculations by *Haqq-* 400  
*Misra et al.* [2008] show that the required concentrations of 401  
 $\text{CH}_4$  are larger than previously believed. Also the  $\text{CH}_4$  402  
 greenhouse effect is limited by the formation of a reflective 403  
 organic haze when  $\text{CH}_4/\text{CO}_2$  is higher than  $\sim 1$ . 404

[22] In this section, we will show calculations with a thin 405  
 cirrus cloud feedback as the one previously described, 406  
 operating at the same time as an atmosphere with larger 407  
 $\text{CO}_2$  concentrations. We perform the same runs as in the 408  
 control case for three different  $\text{CO}_2$  concentrations for  $S =$  409  
 $0.8 S_0$ . The longwave parameterization by *Chou et al.* 410  
 [2002] is deemed appropriate even for concentrations of 411  
 about 100 times present atmospheric levels of  $\text{CO}_2$ . 412

[23] Figure 2 shows the surface temperature for three 413  
 different  $\text{CO}_2$  concentrations at  $S = 0.8 S_0$ . We see that for 414  
 the current climate value of  $f = 0.16$  (vertical dashed grey 415  
 line) and for the present value of  $\text{CO}_2$  (1 PAL), the surface 416  
 temperature is about  $266 \text{ K}$ . For a constant cloud coverage 417

t1.1 **Table 1.** Value of the Cloud Microphysical and Radiative Properties for the Sensitivity Runs<sup>a</sup>

t1.2	cwc ( $10^{-4}$ g/g)	IWP (g/m <sup>2</sup> )	$\tau$	$r_e$ ( $\mu$ m)	LW (W/m <sup>2</sup> )	SW (W/m <sup>2</sup> )	NET (W/m <sup>2</sup> )
t1.3	7	46	1.3	59	120	-70	50
t1.4	3.5	23	0.73	52	70	-35	35
t1.5	28	185	4	75	140	-130	10

<sup>a</sup>Abbreviations: cwc, cloud water content;  $\tau$ , visible optical depth; and LW, SW, and NET, the cloud radiative forcing in the longwave, shortwave, and net, respectively. For all runs the thickness of the cloud is fixed at  $\sim 200$  m, and the cloud is located at 200 hPa.

t1.6

418 the amount of CO<sub>2</sub> required for mean global temperatures to  
 419 rise above 273 is about 20 PAL CO<sub>2</sub>. We recover here the  
 420 well-known result that the paradox cannot be solved solely  
 421 on the basis of a higher concentration of CO<sub>2</sub>, without  
 422 getting a result inconsistent with the paleosol data. If we  
 423 focus on values of CO<sub>2</sub> allowed by the paleosol constraints,  
 424 a solution to the paradox can be found with relatively small  
 425 values for the cloud feedback magnitude. For instance, for  
 426 1 PAL CO<sub>2</sub>, the tropical coverage required to solve the  
 427 paradox is about 1. For the case in which CO<sub>2</sub>  $\sim$  10 PAL,  
 428 the paradox can be solved with a tropical coverage of only  
 429 0.35 and the magnitude of the cloud rate of change required  
 430 for providing these cloud coverage is  $\gamma \sim -5\%/K$ . This  
 431 solution is just barely consistent with the paleosol constraint  
 432 and of course stronger values of the cloud feedback could  
 433 solve the paradox for lower levels of CO<sub>2</sub>. We stress that  
 434 both consistency with the paleosol data and global mean  
 435 temperatures above freezing can be achieved (at least for  
 436 this particular value of solar insolation) invoking only a  
 437 small magnitude of the cloud rate of change. We also note  
 438 that while cirrus coverage is less than full, the effect of  
 439 further increasing cirrus coverage in the mean temperature  
 440 is mostly linear with cloud coverage as opposed to the effect  
 441 of the increase in CO<sub>2</sub> (or other greenhouse gases) in the  
 442 mean temperature that are only logarithmic.

### 3.4. Sensitivity to Cloud Water Content

443

[24] Our results so far, have been obtained with a single  
 444 cloud with optical depth 1.3. We explore the sensitivity to  
 445 changes in the cloud water content of the cloud. Table 1  
 446 summarizes the cloud properties of the different clouds. The  
 447 cloud radiative effects were calculated with the runs  
 448 corresponding to  $f = 0.2$ . The clouds with either much  
 449 larger or much smaller cloud water content than the control  
 450 case produce smaller net radiative effects. Even though  
 451 there is a net positive cloud radiative effect for the cwc  
 452 (cloud water content) =  $28 \times 10^{-4}$  run, the cloud radiative  
 453 effect becomes negative for higher cloud fractions and  
 454 temperatures decrease with cloud coverage (Figure 3b).  
 455 For the thinner cloud case, the net radiative effect is smaller  
 456 but positive and very similar to the control case (Figure 3a).  
 457 This “optimal” net radiative for the control case coincides  
 458 with the ordering provided by *Choi and Ho* [2006] with  
 459 respect to shortwave optical depth; smaller positive radiative  
 460 effect for thinner clouds and smaller and even negative  
 461 radiative effects for thicker clouds.  
 462

### 3.5. Sensitivity to the Fixed Height Assumption

464

[25] We have also tested the possibility that the results are  
 465 sensitive to the assumption of a fixed height or fixed  
 466 pressure level cloud. An alternative to specifying the cloud  
 467 at a constant pressure level is the fixed anvil temperature  
 468 proposed by *Hartmann and Larson* [2002]. They propose  
 469 that the level at which radiative cooling decreases substan-  
 470 tially is controlled by the distribution of water vapor. At the  
 471 same time, the total amount of water vapor is a strong  
 472 function of temperature as a consequence of the Clausius-  
 473 Clapeyron relation. Therefore, radiative cooling rates in the  
 474 troposphere are a strong function temperature (as long as  
 475 water vapor is the main driver of the radiative cooling). The  
 476 divergence of the radiative cooling would then occur at  
 477 about the same temperature no matter the surface temper-  
 478 ature of the climate considered. Since convective heating  
 479 balances radiative cooling in the tropical free troposphere,  
 480

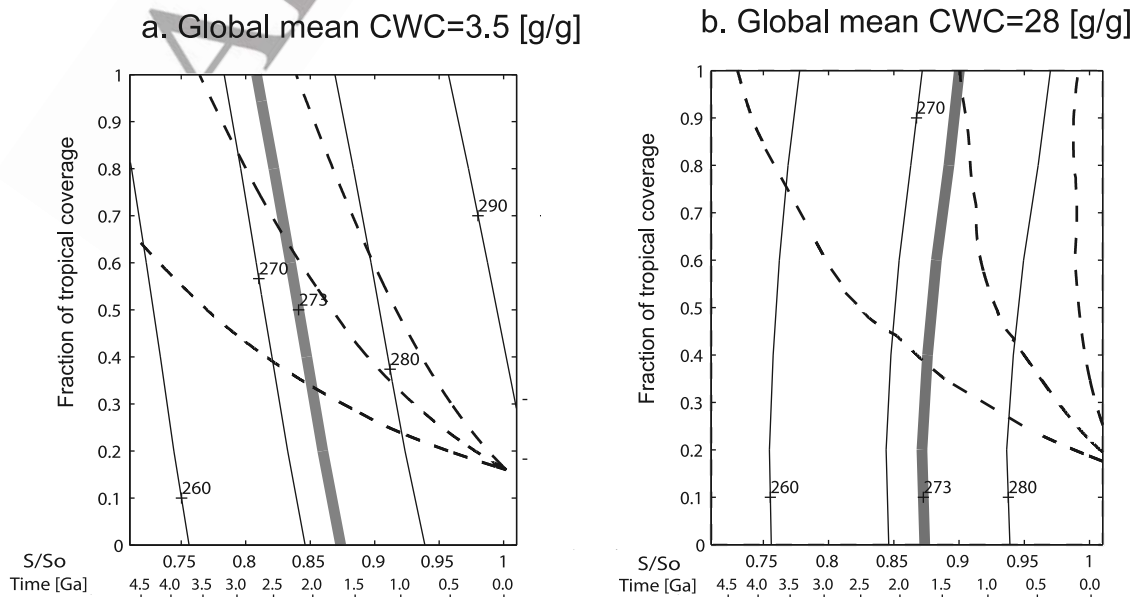


**Figure 3.** Same as Figure 1d but for clouds with different cloud water content: (a) 3.5 g/g and (b) 28 g/g.

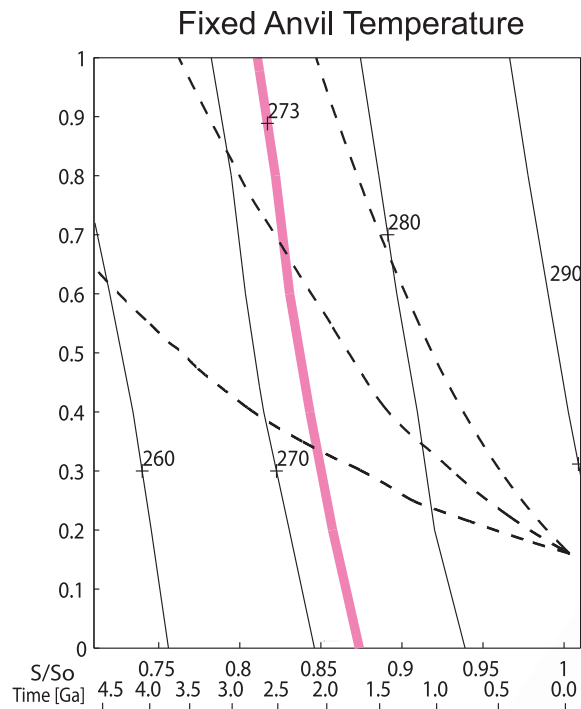


**Figure 4.** Same as Figure 1d but for a fixed temperature anvil cloud at the 220 K level.

481 the level at which convection detrains would be strongly  
 482 constrained to be near a fixed temperature. In Figure 4 we  
 483 show the results for the global mean surface temperature for  
 484 the two-column model in the case in which the cloud is  
 485 located at the 220 K level (this is done iteratively at each  
 486 time step in the tropical column). The results show that the  
 487 magnitude of the cloud effect is only modestly reduced. For  
 488 instance for  $S = 0.81 S_0$ , the tropical coverage required for  
 489 global mean temperatures to be above 273 K in the control  
 case is  $f \gtrsim 0.87$ . For the fixed anvil temperature case  $f \sim 1$ .

### 491 3.6. Sensitivity to Water Vapor Feedback

492 [26] So far we have followed the customary assumption  
 493 of a constant relative humidity profile. In the context of our  
 494 1-D single column tropical model, the assumption of strict  
 495 relative humidity invariance gives a water vapor feedback  
 496 factor,  $\beta \sim 0.4$ . Recent studies suggest that the strong  
 497 positive water vapor feedback implied by the invariance  
 498 of relative humidity may be within reasonable agreement  
 499 with satellite observations [Dessler *et al.*, 2008], even  
 500 though the vertical profile of relative humidity is not strictly  
 501 conserved [see also Sun and Held, 1996]. Renno *et al.*  
 502 [1994], for instance, showed in the context of a radiative-  
 503 convective equilibrium model with an explicit hydrological  
 504 cycle, that changes in the microphysical parameters that  
 505 control the conversion of water to precipitation and vapor  
 506 could produce very different equilibrium climates, with  
 507 different vertical distributions of relative humidity. Since  
 508 we do not have an explicit parameterization for water vapor  
 509 in our model, we specify changes in relative humidity with  
 510 surface temperature to explore the sensitivity of the results  
 511 to the water vapor feedback strength.

[27] We vary the relative humidity in the model from the 512  
 original relative humidity profile according to 513

$$\text{RH}(500 \text{ hPa}) = \alpha \times (T_s - 288) + \text{RH}_0(500 \text{ hPa}), \quad (4)$$

where  $\text{RH}_0$  is the original relative humidity (based on the 514  
 Manabe and Wetherald [1967] profile). Between 200 hPa 516  
 and 800 hPa, the humidity profile is interpolated from the 517  
 original profile to the new value at 500 hPa using a cubic 518  
 spline. Since we have specified the change in the feedback 519  
 in terms of a change in relative humidity, the magnitude of 520  
 the feedback will have a dependence on temperature. We 521  
 use the model output to calculate the magnitude of the water 522  
 vapor feedback for each case. Figure 5 shows the 523  
 temperature dependence of the feedback factor for three 524  
 different values of  $\alpha = -0.015, 0, +0.015$ . The feedback 525  
 factor decreases with temperature for all cases. For the 526  
 imposed changes in relative humidity, the spread of the 527  
 water vapor feedback tends to decrease with temperature. 528  
 This is already an indication that uncertainties in the water 529  
 vapor feedback factor for current climate will be less 530  
 consequential in determining the temperature for lower 531  
 global mean surface temperatures. 532

[28] Figure 6 shows the mean surface temperature for 533  
 two-column model as a function of the cloud fraction for 534  
 $S = 0.8 S_0$ . Global mean temperatures  $\sim 273$  K, are found at 535  
 $f \sim 1$ . Changing  $\alpha$  from  $-0.015/\text{K}$  to  $0.015/\text{K}$  has little 536  
 effect on the total cirrus cloud cover needed for temper- 537  
 atures above freezing. Figure 6 also hints to the fact that 538  
 changes in water vapor feedback are more efficient for 539  
 relatively low cloud coverage, since changes in water vapor 540  
 in the free troposphere are buffered by the presence of the 541  
 cloud above (notice the shaded regions in Figure 6 showing 542  
 the reduced range of variation in  $f$  required for a given 543  
 temperature for low coverage). The two effects, namely the 544  
 decrease in strength of the feedback with temperature and 545

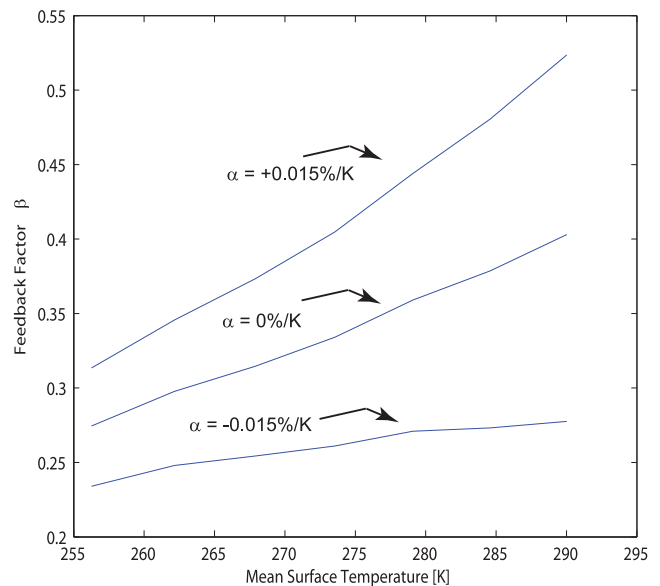


**Figure 5.** Water vapor feedback factor  $\beta$  as a function of temperature for three different values of the strength of the relative humidity change in equation (4) ( $\alpha = -0.015, 0$ , and  $0.015$ ).

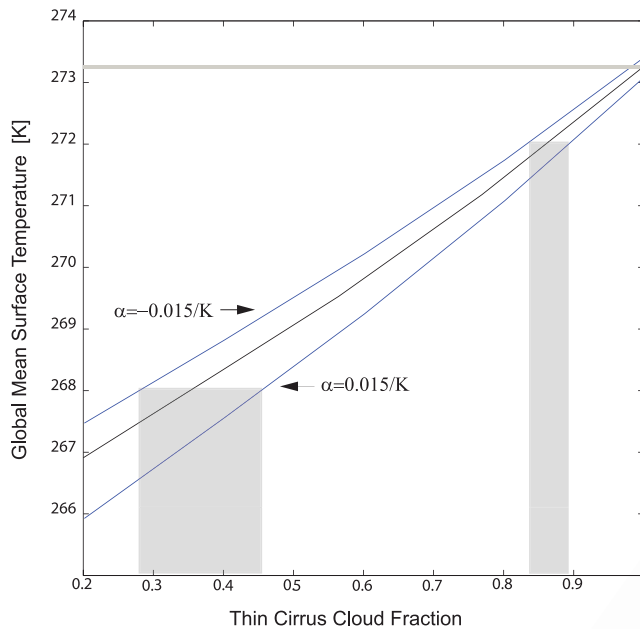


**Figure 6.** Sensitivity of the results for  $S = 0.8S_0$  to the water vapor feedback strength. The two shaded regions show the value of the cloud coverage required to obtain a given global mean temperature (in this case 268 and 272 K).

546 the decrease in strength of the feedback for large cirrus  
547 coverage, suggest that the range of the solution has a low  
548 sensitivity to the strength of the water vapor feedback in the  
549 context of the present model.

### 550 3.7. Sensitivity to the Meridional Heat Flux

551 [29] We have so far assumed a linear diffusivity law for  
552 the heat transport between the tropical and extratropical  
553 column. An alternative to the simple linear diffusivity  
554 would be to assume a constant temperature difference  
555 between the two columns so as to crudely represent a  
556 baroclinic adjustment over the different possible climates  
557 considered [e.g., Stone, 1978]. This is accomplished in the  
558 model by allowing the diffusivity coefficient to change  
559 while keeping a constant target temperature difference  
560 between the two columns (in this case 20 K). In Figure 7  
561 we see the result of this modification. The situation in the  
562 global mean is not very different from the constant diffusivity  
563 depicted in Figure 1d, so that the main result does not  
564 change appreciably; the mean global temperature can be  
565 above freezing for luminosities  $\sim 0.81$  and full tropical  
566 cirrus coverage. However, since in the case of the fixed  
567 temperature difference the tropics are colder than in the  
568 control case (for instance, the mean tropical temperature is  
569 282 K for  $S = 0.81 S_0$  and  $f = 1$  in the fixed meridional  
570 temperature case and 285 K in the linear diffusivity case for  
571 the same conditions) the values of  $\gamma$  required to accomplish  
572 the needed full tropical cirrus coverage are therefore smaller  
573 in the fixed meridional temperature case ( $\gamma \sim -12\%/K$   
574 compared to  $\gamma \sim -15\%/K$  in the control case). By provid-  
575 ing warmer extratropical temperatures, this alternative treat-  
576 ment for the meridional heat flux would also delay the onset  
577 of solutions unstable to an eventual ice-albedo feedback.  
578 Besides the control case and the constant temperature case,

we have a third assumption about the meridional heat 579  
transport. In the case of a single column tropics depicted 580  
in Figure 1 the meridional heat transport is implicit (since 581  
the incoming solar radiation is tuned to obtain current 582  
tropical temperatures) and reduced by the same fraction as 583  
the reduction in incoming solar radiation. In the single 584  
column tropical cases the heat transport becomes less 585  
effective as the climate cools (similar to the decrease in 586  
transport efficiency predicted from maximum entropy con- 587  
siderations [Gerard *et al.*, 1990]). This isolation of the 588  
tropics from the extratropics also allows for a more effective 589  
functioning of the tropical cirrus clouds in resisting the 590  
changes in the solar constant and would provide a more 591  
robust “partial” solution to the paradox, with relatively 592  
warm oceans in the tropical regions of the planet. 593  
594

## 4. Discussion 595

[30] We have presented simplified radiative-convective 596  
equilibrium calculations to investigate the role of thin cirrus 597  
clouds in providing a solution for the faint young Sun 598  
paradox. In the context of our model, solutions do in fact 599  
exist. Tropical thin cirrus clouds can either solve the 600  
paradox in the sense of providing *global* mean temperatures 601  
above freezing (after  $\sim 2.9$  Ga) or in a weaker sense, less 602  
than full tropical cirrus coverage can provide *tropical* mean 603  
temperatures above freezing for all Earth’s existence (in the 604  
context of this model). The solutions are characterized by a 605  
colder tropical temperature and therefore by thin cirrus 606  
clouds acting as a net negative feedback to the solar forcing. 607

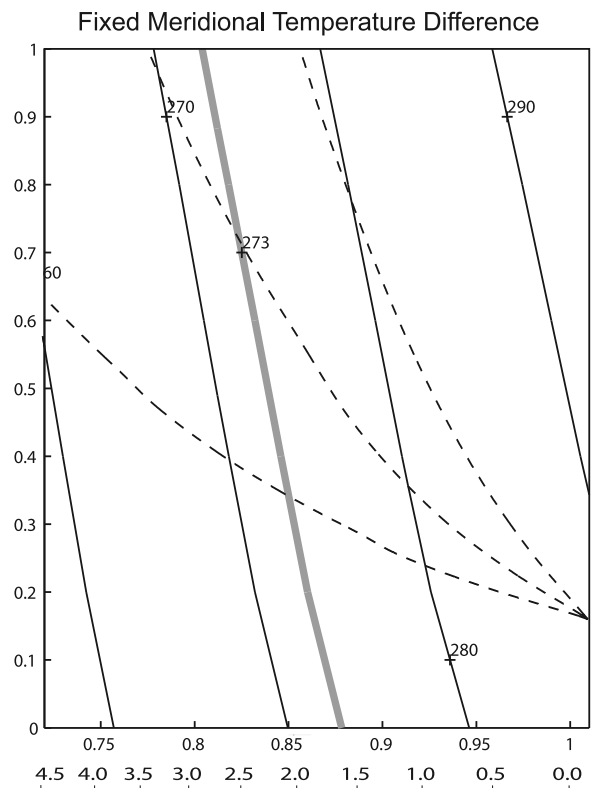


**Figure 7.** Same as Figure 1d but for a fixed difference in surface temperature between the tropical and the extra-tropical column.



[31] Given that thin cirrus clouds can indeed solve the paradox, we focus the discussion on the question of the plausibility of these solutions. There is the suggestion that a negative feedback such as the one required might in fact be operating in current climate [Lindzen *et al.*, 2001]. According to this suggestion, called the iris hypothesis, an increase in sea surface temperature (through an increase in the specific humidity of the air that participates in convection) can make precipitation in convective clouds more efficient. In this way less condensate is rained out from deep convective clouds and therefore more condensate is available to be detrained from the top of the cloud to form cirrus clouds. The iris hypothesis is controversial and it would be lengthy to discuss all the arguments here. Apparent confirmation for the iris effect came from the analysis of the OLR trends over the last two decades, showing a strong increase in the OLR compared to a relatively smaller decrease in the shortwave reflectivity in the tropics [Wielicki *et al.*, 2002; Chen *et al.*, 2002]. Using a combination of data sets, Hatzidimitriou *et al.* [2004] traced the OLR increase mainly to a decrease in the upper level cloud coverage and a drying of the upper troposphere. As pointed out by Chou and Lindzen [2005] this large increase in OLR was also consistent with a much larger value in the relative change in cloud fraction with temperature than the original  $-22\%/K$  found by Lindzen *et al.* [2001]. The OLR trends were recently revised down to only about a quarter of the original value [Wong *et al.*, 2006], although the OLR trend continues to be larger than the Planck response expected from an increase in the tropical mean temperature over the same period. Recently, Lindzen and Choi [2009] studied variations in the outgoing radiative fluxes with respect to changes in the average tropical temperature in intraseasonal scales. A total negative feedback was deduced from the outgoing longwave response of the tropics. If a strong positive water vapor feedback is realistic [e.g., Dessler *et al.*, 2008], then the combined effect of water vapor feedback and lapse rate feedback must be more than compensated by a strong unknown process acting on modifying the longwave flux. This process cannot be distinguished from the bulk of the longwave response in the analysis by Lindzen and Choi [2009], but it most likely resides in the combined behavior of clouds and water vapor in the tropics. This leaves open the possibility that a negative feedback such as the iris is operating in the present climate.

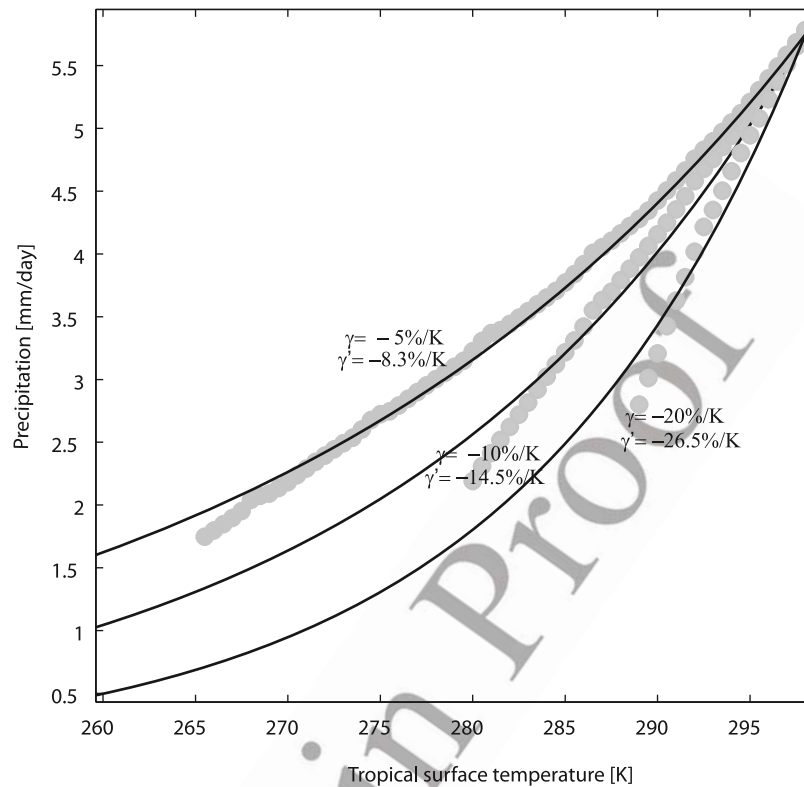
[32] We have assumed so far that the magnitude of the cloud changes with respect to temperature is absolute, that is, they already contain any possible dependence on changes in convective activity that will arise as the incoming radiation at the surface decreases. Theoretical arguments and model simulations both indicate that changes in precipitation with global mean temperature are relatively small ( $\sim 2\text{--}4\%/K$  [Held and Soden, 2006; O’Gorman and Schneider, 2008]). A correction to account for the reduction of precipitation or convective activity will indeed be required. One can diagnose from the surface budget, the total convective heating in the model, which, in the tropics has to be equal to the precipitation. The changes in precipitation in the model depend on the magnitude of the feedback itself, given that a stronger feedback would reduce the net incoming solar radiation at the surface more rapidly than in the case of a weaker feedback. This is illustrated in

Figure 8 which shows the increase in precipitation with temperature for three different values of the absolute cloud change  $\gamma$ . One can write  $\gamma = \gamma' + \frac{1}{P} \frac{\partial P}{\partial T}$ , so that the relative changes in cloud fraction  $\gamma'$ , have to be higher in magnitude than the magnitude of the change  $\gamma$  required to compensate for the decrease of precipitation in a colder climate. Fitting exponential functions to the model-diagnosed precipitation one finds that the quantity  $\frac{1}{P} \frac{\partial P}{\partial T}$  goes from about  $3\%/K$  to  $7\%/K$ .

[33] Regarding observed value of  $\gamma'$ , different data sets and analyses point to values between  $-2\%/K$  to  $-22\%/K$  for current climate (see R. Rondanelli and R. S. Lindzen, Comments on “Variations of tropical upper tropospheric clouds with sea surface temperature and implications for radiative effects,” submitted to *Journal of Geophysical Research*, 2010) for a discussion of some of the methodological issues involved). These empirically derived rates of change  $\gamma'$ , usually refer to some observable that is a proxy for the thin cirrus clouds rather than the thin cirrus clouds themselves. Nevertheless, the magnitude of these changes is consistent with what is required to solve the paradox (for instance from Figures 1c and 1d, the tropical temperature for  $S = 0.8 S_0$  and  $f = 1$  is about 285 K which gives a rate of change of  $\gamma \sim -15\%/K$ ,  $\gamma' \sim -20\%/K$ ).

[34] One can ask what happens in the situation in which the tropical atmosphere is already completely covered by cirrus clouds and temperatures continue to decrease. One could expect that if the cloud feedback still operates beyond full coverage, an increase in the cloud water content or in the thickness of the cirrus clouds would ensue. The cloud feedback can only operate until the cloud is thick enough ( $\tau \sim 10$ ) that surface cooling instead of heating is obtained (as in Figure 3b). At the same time, if the cloud cover is thick enough to reflect most of the incoming solar radiation, convection (and therefore the source of the cloud) will shut off. Microphysical effects such as an enhanced precipitation from the cirrus cloud might prevent this from happening. However, without a mechanistic model one cannot go beyond speculation on this point. We only note here that the mechanism such as the one described will have a limit for low temperatures. The availability of water for sustaining a total cirrus coverage does not pose a problem. Even with a weaker hydrological cycle as expected in a colder climate (rainfall rate estimated in  $\sim 2$  mm/d for a surface temperature of  $\sim 270$  K [O’Gorman and Schneider, 2008]) and with a  $44$  g/m<sup>2</sup> cloud (with an accompanying water vapor layer of  $400$  g/m<sup>2</sup>) and assuming that a typical ice particle dissipates over a day, the detrainment flux required to sustain such a cloud is only about  $\sim 2\%$  of the precipitation rate.

[35] Although the literature about the paradox usually focuses on greenhouse gas solutions [Kasting and Catling, 2003; Shaw, 2008], solutions based on cloud feedbacks have been put forth in the past. Based on the model developed by Wang *et al.* [1981] in which cloud cover is considered proportional to the convective heating (or total precipitation), Rossow *et al.* [1982] [see also McGuffie and Henderson-Sellers, 2005, section 4.6.1] proposed a solution to the paradox based on the negative feedback resulting from a decrease in planetary albedo and a decrease in the cloud water content (and therefore in the visible optical depth) of clouds in a colder climate. Our solution on the



**Figure 8.** Changes in precipitation diagnosed from the surface balance in the tropical column of the model. The gray dots show the precipitation diagnosed from the model for three values of the magnitude of the feedback  $\gamma = 5, 10,$  and  $20\%/K$ . The black lines are exponential fits to the precipitation curves from which a value of  $\gamma'$  was deduced.

732 other hand leaves the albedo almost unchanged as it mostly  
 733 depends on the longwave radiative effect of upper level thin  
 734 cirrus clouds. The solution by *Rossow et al.* [1982] and our  
 735 solution are not mutually exclusive. Several cloud feed-  
 736 backs other than the one resulting from the change in thin  
 737 cirrus are possible in reality and have been muted in the  
 738 present model (for instance area coverage and composition  
 739 of stratocumulus clouds in the subtropics). Despite progress  
 740 since the time of the writing of the study by *Rossow et al.*  
 741 [1982], clouds continue to be “the major source of uncer-  
 742 tainty” in climate models [e.g., *Schwartz, 2008*]. As in  
 743 previous studies dealing with clouds and the faint young  
 744 Sun problem (*Cogley and Henderson-Sellers* [1984] pro-  
 745 vide references to previous work on this issue) (see also the  
 746 mechanism proposed by *Shaviv* [2003]), we conclude that a  
 747 negative cloud feedback can indeed solve the paradox if the  
 748 Archean climate was somewhat colder than present. (How  
 749 much colder will also depend on the strength of the  
 750 feedback.) We have followed the customary assumptions  
 751 of neglecting the ice-albedo feedback, fixing the relative  
 752 humidity and muting the effect of clouds to a large extent,  
 753 we have also assumed a very simplified treatment for the  
 754 heat transport between tropics and extratropics. None of  
 755 these assumptions is entirely satisfactory. Given the simpli-  
 756 fied nature of this radiative-convective model, our study is  
 757 only exploratory.

758 [36] Solving the paradox down to a luminosity of  $S =$   
 759  $0.8 S_0$ , requires a climate with an equilibrium sensitivity  
 760 parameter to solar forcing  $\lambda = \Delta T_s / \Delta S$  of about  $0.29 \text{ K/}$

$(\text{W m}^{-2})$ . This sensitivity value is certainly smaller than 761  
 any of the sensitivities to  $\text{CO}_2$  forcing in current GCMs 762  
 [*Intergovernmental Panel on Climate Change, 2007*], but it 763  
 is within the lower range of estimates made from observa- 764  
 tions [e.g., *Schwartz, 2008*]. One finds values of  $\lambda \sim 0.4 \text{ K/}$  765  
 $(\text{W m}^{-2})$  for the 1-D radiative-convective models without 766  
 clouds (using for instance the results by *Kasting* [1987]); we 767  
 also found a nearly identical value for  $\lambda$  in our two-column 768  
 radiative convective model with no cloud feedback. As 769  
 shown in section 3.3, small changes in the rate of change 770  
 of cloud coverage can reduce the amount of greenhouse 771  
 gases needed to reach consistency with the geological 772  
 evidence. These clouds changes are associated with small 773  
 changes in the model climate sensitivity (a  $-5\%/K$  rate of 774  
 change in the thin cirrus coverage is equivalent to a 775  
 sensitivity  $\lambda \sim 0.37 \text{ K}/(\text{W m}^{-2})$ ) in the present model). 776

## 5. Concluding Remarks

777

[37] Using simple radiative-convective simulations we 778  
 have tested the idea that a coverage of tropical cirrus clouds 779  
 much larger than present could resolve the faint young Sun 780  
 paradox. We have found that relatively modest cloud 781  
 changes can indeed provide sufficient cirrus coverage for 782  
 the mean global temperature to be above freezing for  $S \gtrsim$  783  
 $0.8 S_0$  and for the mean tropical temperature to be above 784  
 freezing for  $S \gtrsim 0.7 S_0$  without additional greenhouse gases. 785  
 The model cloud is specified to have similar cloud radiative 786  
 effect as reported in current climate observations. We tested 787

788 the sensitivity of the results to cloud water content, to the  
789 assumption of a constant pressure level of detrainment and  
790 to a range for the strength of the water vapor feedback. We  
791 also looked at two different treatments for the meridional  
792 heat transport. We find small sensitivities to all these factors  
793 in the present model. Although we describe a very specific  
794 cloud negative feedback, our results can be understood in a  
795 more general perspective with respect to the faint young  
796 Sun paradox; a moderate negative climate feedback can  
797 indeed resolve the paradox without resorting to large  
798 changes in the greenhouse gas content of the Archean  
799 atmosphere.

800 [38] **Acknowledgments.** We thank M.D. Chou for providing us with  
801 the radiative code used in this study. Comments by Yong-Sang Choi and  
802 Jacob Haqq-Misra on earlier versions of the manuscript are appreciated. We  
803 also appreciate a thoughtful review by Dorian Abbott and comments from  
804 two anonymous reviewers that helped to improve the manuscript.

## 805 References

- 806 Catling, D., and J. Kasting (2007), Planetary atmospheres and life, in  
807 *Planets and Life: The Emerging Science of Astrobiology*, pp. 91–116,  
808 Cambridge Univ. Press, Cambridge, U. K.
- 809 Chen, J., B. Carlson, and A. Del Genio (2002), Evidence for strengthening  
810 of the tropical general circulation in the 1990s, *Science*, 295(5556), 838–  
811 841.
- 812 Choi, Y.-S., and C.-H. Ho (2006), Radiative effect of cirrus with different  
813 optical properties over the tropics in MODIS and CERES observations,  
814 *Geophys. Res. Lett.*, 33, L21811, doi:10.1029/2006GL027403.
- 815 Chou, M., and R. Lindzen (2005), Comments on “Examination of the  
816 decadal tropical mean ERBS nonscanner radiation data for the iris  
817 hypothesis,” *J. Clim.*, 18(12), 2123–2127.
- 818 Chou, M., and M. Suarez (2002), A Solar Radiation parameterization for  
819 atmospheric studies, *NASA Tech. Memo, TM-1999-10460*, vol. 15, 52 pp.
- 820 Chou, M., K. Lee, S. Tsay, and Q. Fu (1999), Parameterization for cloud  
821 longwave scattering for use in atmospheric models, *J. Clim.*, 12(1), 159–  
822 169.
- 823 Chou, M., K. Lee, and P. Yang (2002), Parameterization of shortwave cloud  
824 optical properties for a mixture of ice particle habits for use in atmo-  
825 spheric models, *J. Geophys. Res.*, 107(D21), 4600, doi:10.1029/  
826 2002JD002061.
- 827 Chou, M. D., M. J. Suarez, X.-Z. Liang, and M. M.-H. Yan (2003), A  
828 Thermal Infrared Radiation Parameterization for Atmospheric studies,  
829 *NASA Tech. Memo, TM-2001-104606*, vol. 19, 55pp.
- 830 Cogley, J., and A. Henderson-Sellers (1984), The origin and earliest state of  
831 the Earth’s hydrosphere, *Rev. Geophys.*, 22(2), 131–175.
- 832 Dessler, A. E., Z. Zhang, and P. Yang (2008), Water-vapor climate feedback  
833 inferred from climate fluctuations, 2003–2008, *Geophys. Res. Lett.*, 35,  
834 L20704, doi:10.1029/2008GL035333.
- 835 Emanuel, K. A. (2007), Quasi-equilibrium dynamics of the tropical atmo-  
836 sphere, in *The Global Circulation of the Atmosphere*, pp. 186–218,  
837 Princeton Univ. Press, Princeton, N. J.
- 838 Endal, A., and K. Schatten (1982), The faint young Sun-climate paradox:  
839 Continental influences, *J. Geophys. Res.*, 87, 7295–7302.
- 840 Gerard, J., D. Delcourt, and L. Francois (1990), The maximum entropy  
841 production principle in climate models: Application to the faint young  
842 Sun paradox, *Q. J. R. Meteorol. Soc.*, 116, 1123–1132, doi:10.1256/  
843 smsj.49505.
- 844 Gough, D. (1981), Solar interior structure and luminosity variations, *Sol.*  
845 *Phys.*, 74(1), 21–34.
- 846 Haqq-Misra, J. D., S. D. Domagal-Goldman, P. J. Kasting, and J. F. Kasting  
847 (2008), A revised, hazy methane greenhouse for the Archean Earth,  
848 *Astrobiology*, 8(6), 1127–1137, doi:10.1089/ast.2007.0197.
- 849 Hart, M. (1978), The evolution of the atmosphere of the Earth, *Icarus*, 33,  
850 23–39.
- 851 Hartmann, D., and K. Larson (2002), An important constraint on tropical  
852 cloud–climate feedback, *Geophys. Res. Lett.*, 29(20), 1951, doi:10.1029/  
853 2002GL015835.
- 854 Hatzidimitriou, D., I. Vardavas, K. Pavlakis, N. Hatzianastassiou,  
855 C. Matsoukas, and E. Drakakis (2004), On the decadal increase in the  
856 tropical mean outgoing longwave radiation for the period 1984–2000,  
857 *Atmos. Chem. Phys.*, 4, 1419–1425.
- 858 Held, I., and B. Soden (2006), Robust responses of the hydrological cycle  
859 to global warming, *J. Clim.*, 19(21), 5686–5699.
- Henderson-Sellers, A., and J. G. Cogley (1982), The Earth’s early hydro- 860  
sphere, *Nature*, 298, 832–835. 861
- Intergovernmental Panel on Climate Change (2007), *Climate Change 2007:* 862  
*The Physical Science Basis*, edited by S. Solomon et al., Cambridge Univ. 863  
Press, Cambridge, U. K. 864
- Kasting, J. (1987), Theoretical constraints on oxygen and carbon dioxide 865  
concentrations in the Precambrian atmosphere, *Precambrian Res.*, 34(3–4), 866  
205–229. 867
- Kasting, J. (1993), Earth’s early atmosphere, *Science*, 259(5097), 920–926. 868
- Kasting, J., and D. Catling (2003), Evolution of a habitable planet, *Annu.* 869  
*Rev. Astron. Astrophys.*, 41, 429–463. 870
- Kasting, J., O. Toon, and J. Pollack (1988), How climate evolved on the 871  
terrestrial planets, *Sci. Am.*, 258(2), 90–97. 872
- Kuhn, W., and S. Atreya (1979), Ammonia photolysis and the greenhouse 873  
effect in the primordial atmosphere of the Earth, *Icarus*, 37, 207–213. 874
- Lindzen, R. S., and Y.-S. Choi (2009), On the determination of climate 875  
feedbacks from ERBE data, *Geophys. Res. Lett.*, 36, L16705,  
doi:10.1029/2009GL039628. 877
- Lindzen, R., and B. Farrell (1980), The role of polar regions in global 878  
climate, and a new parameterization of global heat transport, *Mon. Weather* 879  
*Rev.*, 108(12), 2064–2079. 880
- Lindzen, R. S., M.-D. Chou, and A. Y. Hou (2001), Does the Earth have an 881  
adaptive infrared iris?, *Bull. Am. Meteorol. Soc.*, 82(3), 417–432. 882
- Liou, K. (2005), Cirrus clouds and climate, in *Yearbook of Science and* 883  
*Technology*, pp. 51–53, McGraw-Hill, New York. 884
- Liou, K., and K. Gebhart (1982), Numerical experiments on the thermal 885  
equilibrium temperature in cirrus cloudy atmospheres, *J. Meteorol. Soc.* 886  
*Jpn.*, 60, 570–582. 887
- Lovelock, J., and M. Whitfield (1982), Life span of the biosphere, *Nature*, 888  
296, 561–563. 889
- Mace, G., M. Deng, B. Soden, and E. Zipser (2006), Association of tropical 890  
cirrus in the 10–15-km layer with deep convective sources: An observa- 891  
tional study combining millimeter radar data and satellite-derived trajec- 892  
tories, *J. Atmos. Sci.*, 63(2), 480–503. 893
- Manabe, S., and R. Strickler (1964), Thermal equilibrium of the atmosphere 894  
with a convective adjustment, *J. Atmos. Sci.*, 21(4), 361–385. 895
- Manabe, S., and R. Wetherald (1967), Thermal equilibrium of the atmo- 896  
sphere with a given distribution of relative humidity, *J. Atmos. Sci.*, 24(3), 897  
241–259. 898
- McFarquhar, G. (2001), Comments on ‘Parametrization of effective sizes of 899  
cirrus-cloud particles and its verification against observations’ by Zhian 900  
Sun and Lawrie Rikus (October B, 1999, 125, 3037–3055), *Q. J. R.* 901  
*Meteorol. Soc.*, 127, 261–266. 902
- McGuffie, K., and A. Henderson-Sellers (2005), *A Climate Modelling* 903  
*Primer*, John Wiley, Hoboken, N. J. 904
- Minton, D., and R. Malhotra (2007), Assessing the massive young Sun 905  
hypothesis to solve the warm young Earth puzzle, *Astrophys. J.*, 906  
660(2), 1700–1706. 907
- Newman, M., and R. Rood (1977), Implications of solar evolution for the 908  
Earth’s early atmosphere, *Science*, 198(4321), 1035–1037. 909
- O’Gorman, P., and T. Schneider (2008), The hydrological cycle over a wide 910  
range of climates simulated with an idealized GCM, *J. Clim.*, 22(21), 911  
5676–5685, doi:10.1175/2009JCLI2701.1. 912
- Owen, T., R. Cess, and V. Ramanathan (1979), Enhanced CO<sub>2</sub> greenhouse 913  
to compensate for reduced solar luminosity on early Earth, *Nature*, 277, 914  
640–642. 915
- Paltridge, G. (1978), The steady-state format of global climate, *Q. J. R.* 916  
*Meteorol. Soc.*, 104, 927–945. 917
- Pavlov, A., J. Kasting, L. Brown, K. Rages, and R. Freedman (2000), 918  
Greenhouse warming by CH<sub>4</sub> in the atmosphere of early Earth, *J. Geo-* 919  
*phys. Res.*, 105, 11,981–11,990. 920
- Pavlov, A., M. Hurtgen, J. Kasting, and M. Arthur (2003), Methane-rich 921  
Proterozoic atmosphere?, *Geology*, 31(1), 87–90. 922
- Pierrehumbert, R. T. (2010), *Principles of Planetary Climate*, Cambridge 923  
Univ. Press, Cambridge, U. K. 924
- Pinti, D. (2005), The origin and evolution of the oceans, in *Lectures in* 925  
*Astrobiology*, vol. 1, edited by M. Gargaud et al., pp. 83–111, Springer, 926  
New York. 927
- Renno, N., K. Emanuel, and P. Stone (1994), Radiative-convective model 928  
with an explicit hydrologic cycle: 1. Formulation and sensitivity to model 929  
parameters, *J. Geophys. Res.*, 99, 14,429–14,442, doi:10.1029/  
94JD00020. 930
- Rollinson, H. (2007), *Early Earth Systems: A Geochemical Approach*, 932  
Blackwell, Malden, Mass. 933
- Rossow, W., A. Henderson-Sellers, and S. Weinreich (1982), Cloud feed- 934  
back: A stabilizing effect for the early Earth?, *Science*, 217(4566), 1245– 935  
1247. 936
- Rye, R., P. Kuo, and H. Holland (1995), Atmospheric carbon dioxide con- 937  
centrations before 2.2 billion years ago, *Nature*, 378, 603–605. 938

- 939 Sackmann, I., and A. Boothroyd (2003), Our Sun: V. A bright young Sun  
940 consistent with helioseismology and warm temperatures on ancient Earth  
941 and Mars, *Astrophys. J.*, 583(2), 1024–1039.
- 942 Sagan, C., and G. Mullen (1972), Earth and Mars: Evolution of atmo-  
943 spheres and surface temperatures, *Science*, 177(4043), 52–56.
- 944 Sassen, K., Z. Wang, and D. Liu (2008), Global distribution of cirrus clouds  
945 from CloudSat/Cloud-Aerosol Lidar and Infrared Pathfinder Satellite  
946 Observations (CALIPSO) measurements, *J. Geophys. Res.*, 113,  
947 D00A12, doi:10.1029/2008JD009972.
- 948 Schwartz, S. (2008), Uncertainty in climate sensitivity: Causes, conse-  
949 quences, challenges, *Energy Environ. Sci.*, 1(4), 430–453.
- 950 Schwartzman, D., and T. Volk (1989), Biotic enhancement of weathering  
951 and the habitability of Earth, *Nature*, 340, 457–460.
- 952 Schwartzman, D., and T. Volk (2004), Does life drive disequilibrium in the  
953 biosphere?, in *Scientists Debate Gaia: The Next Century*, edited by S. H.  
954 Schneider et al., pp. 129–135, MIT Press, Cambridge, Mass.
- 955 Schwarzschild, M. (1958), *Structure and Evolution of the Stars*, Princeton  
956 Univ. Press, Princeton, N. J.
- 957 Shaviv, N. (2003), Toward a solution to the early faint Sun paradox: A  
958 lower cosmic ray flux from a stronger solar wind, *J. Geophys. Res.*,  
959 108(A12), 1437, doi:10.1029/2003JA009997.
- 960 Shaw, G. H. (2008), Earth's atmosphere—Hadean to early Proterozoic,  
961 *Chem. Erde Geochem.*, 68(3), 235–264, doi:10.1016/j.chemer.2008.  
962 05.001.
- 963 Stone, P. (1978), Baroclinic adjustment, *J. Atmos. Sci.*, 35(4), 561–571.
- 964 Sun, D., and I. Held (1996), A comparison of modeled and observed  
965 relationships between interannual variations of water vapor and tempera-  
966 ture, *J. Clim.*, 9(4), 665–675.
- Volk, T. (1987), Feedbacks between weathering and atmospheric CO<sub>2</sub> over 967  
the last 100 million years, *Am. J. Sci.*, 287(8), 763–779. 968
- Walker, J., P. Hays, and J. Kasting (1981), A negative feedback mechanism 969  
for the long-term stabilization of the Earth's surface temperature, *J. Geo-* 970  
*phys. Res.*, 86, 9776–9782. 971
- Wang, W., W. Rossow, M. Yao, and M. Wolfson (1981), Climate sensitivity 972  
of a one-dimensional radiative-convective model with cloud feedback, 973  
*J. Atmos. Sci.*, 38(6), 1167–1178. 974
- Wielicki, B., et al. (2002), Evidence for large decadal variability in the 975  
tropical mean radiative energy budget, *Science*, 295(5556), 841–844. 976
- Wilde, S., J. Valley, W. Peck, and C. Graham (2001), Evidence from detrital 977  
zircons for the existence of continental crust and oceans on the Earth 978  
4.4 Gyr ago, *Nature*, 409, 175–178. 979
- Wong, T., B. Wielicki, R. Lee III, G. Smith, K. Bush, and J. Willis (2006), 980  
Reexamination of the observed decadal variability of the Earth Radiation 981  
Budget using altitude-corrected ERBE/ERBS nonscanner WFOV data, 982  
*J. Clim.*, 19(16), 4028–4040. 983
- Zahnle, K., and N. H. Sleep (2002), Carbon dioxide cycling through the 984  
mantle and implications for the climate of ancient Earth, *Geol. Soc. Spec.* 985  
*Publ.*, 199(1), 231–257, doi:10.1144/GSL.SP.2002.199.01.12. 986

---

R. S. Lindzen and R. Rondanelli, Department of Earth, Atmospheric and 987  
Planetary Sciences, Massachusetts Institute of Technology, 54-1717, 989  
77 Massachusetts Ave., Cambridge, MA 02139, USA. (rondane@mit.edu) 990